JACS
JOURNAL OF THE AMERICAN CHEMICAL SOCIETY
Communication
pubs.acs.org/JACS

Diatom Mimics: Directing the Formation of Biosilica Nanoparticles by Controlled Folding of Lysine-Leucine Peptides

Joe E. Baio,[†] Ariel Zane,[‡] Vance Jaeger,[§] Adrienne M. Roehrich,[‡] Helmut Lutz,[∥] Jim Pfaendtner,[§] Gary P. Drobny,*[,‡] and Tobias Weidner*[,§,∥]

[†]School of Chemical, Biological, and Environmental Engineering, Oregon State University, Corvallis, Oregon 97331, United States
[‡]Department of Chemistry and [§]Department of Chemical Engineering, University of Washington, Seattle, Washington 98195, United States
[∥]Max Planck Institute for Polymer Research, 55128 Mainz, Germany

Supporting Information

ABSTRACT: Silaffins, long chain polyamines, and other biomolecules found in diatoms are involved in the assembly of a large number of silica nanostructures under mild, ambient conditions. Nanofabrication researchers have sought to mimic the diatom's biosilica production capabilities by engineering proteins to resemble aspects of naturally occurring biomolecules. Such mimics can produce monodisperse biosilica nanospheres, but in vitro production of the variety of intricate biosilica nanostructures that compose the diatom frustule is not yet possible. In this study we demonstrate how LK peptides, composed solely of lysine (K) and leucine (L) amino acids arranged with varying hydrophobic periodicities, initiate the formation of different biosilica nanostructures in vitro. When L and K residues are arranged with a periodicity of 3.5 the α-helical form of the LK peptide produces monodisperse biosilica nanospheres. However, when the LK periodicity is changed to 3.0, corresponding to a 3_{10} helix, the morphology of the nanoparticles changes to elongated rod-like structures. β-strand LK peptides with a periodicity of 2.0 induce wire-like silica morphologies. This study illustrates how the morphology of biosilica can be changed simply by varying the periodicity of polar and nonpolar amino acids.

The control of size and shape of silica SiO_2 is relevant for a variety of technical applications including electronics,[1] coatings, cosmetics,[2] catalysis,[3] and medical applications.[4] Although the control of silica morphology by most industrial approaches requires extremes in physical and chemical conditions, there exists in a variety of organisms including marine sponges[5] and diatoms,[6] a form of protein-mediated silica morphogenesis in which highly ordered structures made of silica (i.e., biosilica) are produced under mild, ambient conditions.[7]

Diatoms are the dominant siliceous species in the sense that they produce the largest portion of the earth's biogenic silica, which in total is estimated at 240×10^{12} moles per year.[8] In the silica deposition vesicles (SDV) of diatoms, biomineralization proteins and other organic molecules including long chain polyamines (LCPA's) are believed to assemble into structured aggregates which induce formation of complex silica morphologies from dissolved orthosilicic acid, i.e., $Si(OH)_4$.[6,9−13] One of the first proteins found to play a definitive role in silica morphogenesis in diatoms is silaffin.[9,10] It has been demonstrated that the surface active domain of silaffins, the portion of the protein that binds to SiO_2, consists of a specific sequence of amino acids that are repeated several times. The structure of the precipitated biosilica depends strongly on the sequence of these repeat units,[9,10,12] which consist of regularly spaced lysine-lysine and arginine-arginine clusters. In addition to these basic amino acids clusters, LCPA's are also present in biosilica composites and have been shown to induce formation of a variety of silica morphologies.[13]

Previous strategies to mimic the silica-formation activity of silaffins have been based on assembling biosilica from (i) poly lysine homopeptides;[14,15] (ii) dendermeric poly amines;[13,16] (iii) small peptides with primary sequences identical to the repeat portions of silaffins;[9,16−20] and (iv) templating silica structures with fibril-like peptide aggregates.[21,22] This large body of work demonstrates how a variety of silaffin "mimics" can be applied to the formation of monodisperse biosilica structures and has focused primarily on the production of nanospheres.

In this study we complement this body of knowledge by demonstrating how so-called LK peptides composed solely of lysine (K) and leucine (L) amino acids give rise to a variety of biosilica morphologies. The structural features of silica precipitated by lysine-rich peptides including porosity, surface area, and particle size have been studied thoroughly as a function of the number of lysine amino acids per molecule.[20] Control of biosilica morphology by externally applied forces has also been reported.[19] Here we have shown that overall silica morphology can be drastically altered without markedly varying the length or the number of lysines per molecule and without the use of externally applied forces. Instead, we demonstrate how silica morphology simply can be controlled by varying the periodicity with which lysine and leucine amino acids are displayed in the primary sequence.

We use a class of model peptides called LK peptides which exhibit an alternation of nonpolar L and polar K amino acids

Received: July 31, 2014
Published: October 6, 2014

   dx.doi.org/10.1021/ja5078238 | J. Am. Chem. Soc. 2014, 136, 15134−15137

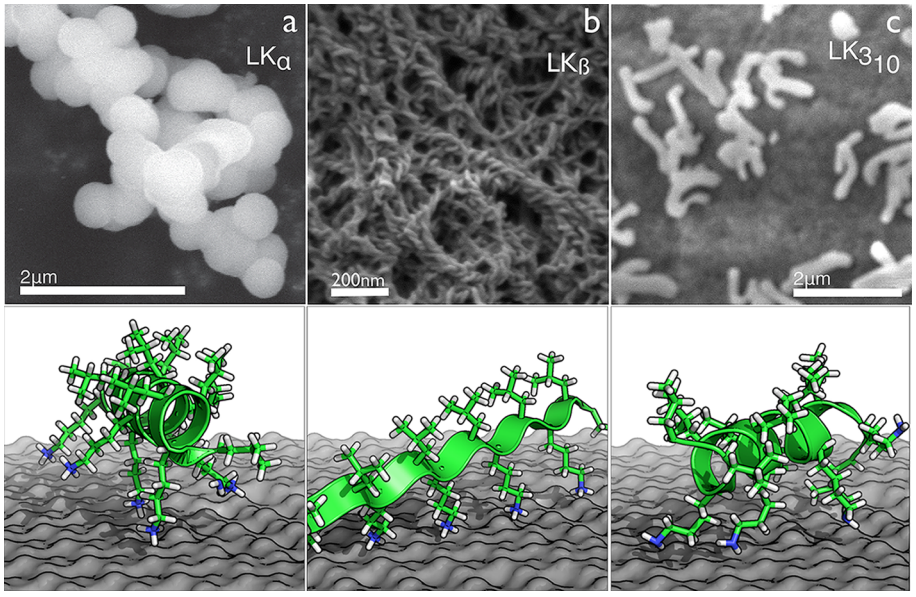

Figure 1. SEM images of the precipitates assembled by the LK peptide mimics. LKα-14, when introduced into a buffer-silicic acid solution, self-assembles silica nanospheres (a). LKβ-15 produces wire-like silica particles with no specific geometry (b), while LK3_{10}-13 induces the formation of monodisperse nanorods (c).

with defined hydrophobic periodicities.[23] The periodicity with which L and K residues are arranged with the peptide directs the formation of particular secondary structures at air−water interfaces[23,24] and on solid, polar, and nonpolar surfaces.[25−28] For example the 14 amino acid LK peptide Ac-LKKLLKLLKKLLKL-COOH (LKα-14) with a periodicity of d = 3.5 assumes an α-helical structure when adsorbed onto solid polymer surfaces.[29,30] LK peptides Ac-LKLKLKLKLKLKL-COOH and Ac-LLKLLKLLKLLKL-COOH have periodicities of 2 and 3, respectively, (i.e., LKβ-15 and LK3_{10}-13) and are designed to fold as β-sheets[16,24] and 3_{10} helices.[23,25,27]

For all three LK peptides, silica precipitate formation was initiated by placing a 5 mg/mL peptide-phosphate buffered saline solution into a silicic acid solution (17% v/v tetramethylorthosilicate in 1 mM HCl). Representative SEMs of the peptide-silica particles formed by the three different LK peptides (Figure 1) illustrate how, depending upon the arrangements of basic and nonpolar amino acids in their primary sequences (i.e., the hydrophobic periodicity), a variety of biosilica nanostructures are formed. For the three cases reported here, the LKα-14 precipitate monodisperse nanospheres, ∼500 nm in diameter (Figure 1A), while the LKβ-15 forms twisted wire-like structures 20 nm in width (Figure 1B). However, when LK3_{10}-13 with periodicity 3.0 is introduced into silicic acid solutions, rod-like structures 100 nm in width and 400 nm long (Figure 1C) are formed.

Because each LK peptide induces a different silica morphology depending on its hydrophobic periodicity, and the hydrophobic periodicity determines the secondary structures of these peptides at a variety of interfaces, the degree to which the secondary structures of LKα-14, LK3_{10}-13, and LKβ-15 are preserved on SiO_2 surfaces was monitored with sum frequency generation vibrational spectroscopy (SFG). SFG spectra at the amide I vibrational band (1550−1750 cm^{-1}) were collected through the backside of a 15 × 15 × 10 mm equilateral CaF_2 prism, where one face of the prism had been coated with a 10 nm layer of SiO_2. This coated face was then immersed into a 5 mg/mL peptide-phosphate buffered saline solution (Figure 2). The SFG selection rules dictate that a SFG

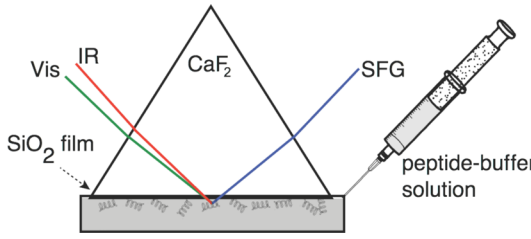

Figure 2. SFG experimental setup. During each experiment peptides (LKα-14, LKβ-15, or LK3_{10}-13) were adsorbed onto a thin layer of SiO_2 (∼10 nm) coated onto the backside of a equilateral CaF_2 prism. In situ SFG spectra collected at the amide I band were used to identify the secondary structure of LKα-14, LKβ-15, and LK3_{10}-13 while interacting with SiO_2.

response will only originate from a surface or interface where inversion symmetry is broken. As a result of these selection rules, any vibrational mode observed within the amide I stretching region will only originate from ordered secondary structures directly interacting with the SiO_2 substrate.

The SFG amide I spectra of the three different LK peptides interacting with the SiO_2 surface are shown in Figure 3. Within the LK3_{10}-13 spectrum is single amide I mode present at 1660 cm^{-1}, which is characteristic of ordered 3_{10} helices.[27] A single peak is also present in the LKα-14 spectrum but is shifted by 5 cm^{-1} to 1655 cm^{-1}, which is attributed to ordered α-helices.[28,31] The LKβ-15 spectrum contains two modes at 1640 and 1670 cm^{-1} which are characteristic of ordered β-sheet structures.[32,33]

In all three cases the secondary structure of the peptides (α-helical, 3_{10}-helical, or β-sheet) are preserved at the SiO_2 surfaces. What is not as obvious is that the silica morphologies induced by the peptides LKα-14 and LK3_{10}-13, both of which display variants of a secondary structure, are markedly different. What is even more interesting is that although LKβ-15

dx.doi.org/10.1021/ja5078238 | J. Am. Chem. Soc. 2014, 136, 15134−15137

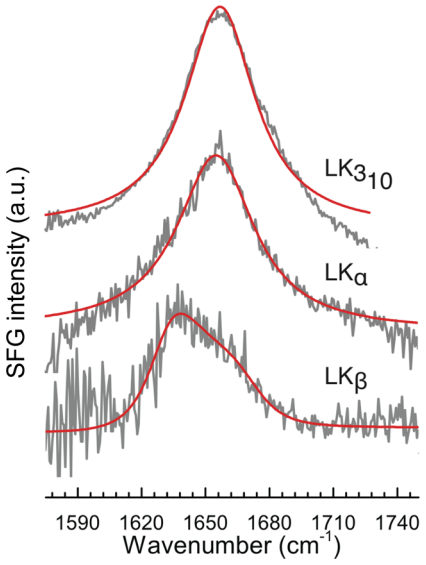

Figure 3. SFG amide I spectra of LK3$_{10}$-13 (top trace) LKα-14 (middle trace), and LKβ-15 (bottom trace) adsorbed onto SiO_2. Within the LK3$_{10}$-13 spectrum is single amide I mode present at 1660 cm^{-1}, which is characteristic of ordered 3$_{10}$ helices. A single peak is also present in the LKα-14 spectrum but is shifted by 5−1655 cm^{-1}, which is attributed to ordered α-helices. The LKβ-15 spectrum contains two modes at 1640 and 1670 cm^{-1}, which are characteristic of ordered β-sheet structures.

structures as a ordered β-strand at silica surfaces, the peptide precipitates twisted, wire-type silica morphologies with little symmetry.

To identify the different mechanisms by which these peptides template the formation of structures with different morphologies, we conducted coarse-grained well-tempered metadynamics simulations of five peptides to elucidate the shape and relative free energy of different aggregated states. The lowest free energy aggregates adopt different conformations (Figure 4)

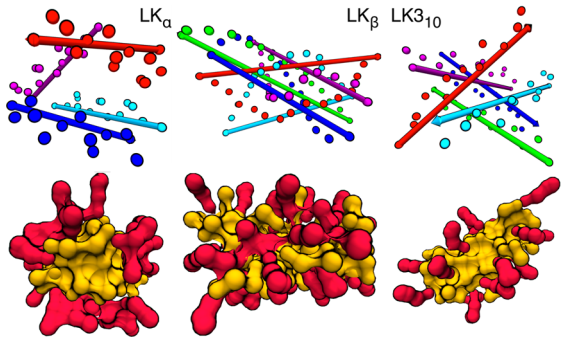

Figure 4. Renderings of low-energy structures from simulations. Figures are not to scale with each other. Vector and bead representations are colored per peptide. Beads represent backbone particles. Vectors are drawn between the ends to guide the eye. Surface representations are colored with hydrophobic leucines in yellow and charged lysines in red.

that can help explain the morphology of the nanostructures seen in the SEM images in Figure 1. The aggregation of the peptides is governed by the attraction of the leucine residues and their tendency to form a hydrophobic core and the repulsion of the charged lysine residues and their tendency to push apart nearby peptides.

For LKβ-15 the lowest free energy structures were those in which all five peptides aggregated with the peptides layered over each other. Vectors drawn between the ends of the peptide backbones show that the peptides lay mostly along one axis, and this gives the aggregates roughly cylindrical structures. Exposed hydrophobic areas tend to be more prevalent at the end of these cylindrical structures, and because the attraction of these peptides and aggregates is based on hydrophobic interactions, the exposed hydrophobic ends should encourage the formation of larger string-like structures.

LK3$_{10}$-13 peptides form a less layered structure with a pill-like aggregate being the lowest energy state. Because of the lower proportion of lysine residues in the peptides, the surfaces of these aggregates are much more hydrophobic than either LKβ-15 or LKα-14. This should encourage the formation of larger aggregates with growth in all three dimensions, leading to larger structures with rod-like shapes.

For LKα-14 there are two similarly energetically favorable low-energy states, a tetramer and a pentamer. The presence of a low-energy tetramer for LKα-14 is consistent with previous experimental studies.[34] The morphology of these aggregates is less layered than the aggregates of LKβ-15 and LK3$_{10}$-13. Instead, the aggregates form rough spheres or hemispheres. Exposed hydrophobic residues are randomly dispersed across the surface of the aggregates, which should encourage the growth in all directions nearly equally, leading to roughly spherical microstructures.

It should be noted that the presented data do not fully explain or prove a specific nucleation mechanism. However, the simple design of the model peptides and the combination of interface spectroscopy, microscopy, and simulations provide a strong basis for the hypothesis that the binding motif and solution aggregation of the peptide dictate the biomineralization process. Specifically, the size and shape of biomimetic SiO_2 particles can be engineered by controlling the backbone folding of biomineralization proteins. This study demonstrates the potential to design biosilica nanomaterials from the ground up. If a particle with a specific shape needs to be fabricated, a peptide with a specific amino acid sequence can be produced that corresponds to that specific geometry. Based on this hypothesis, the final morphology produced is determined by the symmetry and the distribution of hydrophobic and hydrophilic patches of LK aggregates. This approach could be tested by in silico design of new sequences, which fold into aggregates with desired shape and charge distribution and the subsequent analysis of obtained precipitates using SEM. The protein design algorithms for such an experiment already exist. For example, the ROSETTA package has successfully been used to engineer new protein sequences for specific tasks. The next step would be to expand this parameter space and explore whether more complex combinations of different biosilcia morphologies could be engineered by peptides with multiple secondary structures, mixed peptide solutions, or sequential precipitation by introducing different peptides during the biomineralization process.

■ ASSOCIATED CONTENT

Ⓢ Supporting Information

Details of the precipitate preparation, SFG experiments, and MD simulations. This material is available free of charge via the Internet at http://pubs.acs.org.

dx.doi.org/10.1021/ja5078238 | J. Am. Chem. Soc. 2014, 136, 15134−15137

AUTHOR INFORMATION

Corresponding Authors

drobny@chem.washington.edu
weidner@mpip-mainz.mpg.de

Notes

The authors declare no competing financial interest.

ACKNOWLEDGMENTS

T.W. thanks the DFG (WE4478/2-1) and the EU (CIG 1202620) for financial support. J.E.B. thanks the NSF for a research fellowship (1202620). G.P.D. acknowledges NSF grant NSF-CHE-1213432. H.L. and T.W. thank Gunnar Glasser for recording SEM images. J.P. and V.J. acknowledge NSF award CBET-1264459 and the Hyak supercomputer system supported in part by UW-IT.

REFERENCES

(1) López, C. *Adv. Mater.* **2003**, *15*, 1679.
(2) Bowman, D. M.; van Calster, G.; Friedrichs, S. *Nat. Nanotechnol.* **2010**, *5*, 92.
(3) Zeng, H. C. *Acc. Chem. Res.* **2012**, *46*, 226.
(4) Kusaka, T.; Nakayama, M.; Nakamura, K.; Ishimiya, M.; Furusawa, E.; Ogasawara, K. *PloS One* **2014**, *9*, e92634.
(5) Weaver, J. C.; Pietrasanta, L. I.; Hedin, N.; Chmelka, B. F.; Hansma, P. K.; Morse, D. E. *J. Struct. Biol.* **2003**, *144*, 271.
(6) Hildebrand, M. *Chem. Rev.* **2008**, *108*, 4855.
(7) Chen, C. L.; Rosi, N. L. *Angew. Chem., Int. Ed.* **2010**, *49*, 1924.
(8) Wever, P. D.; Dumitriva, P.; Caulet, J. P.; Nigrini, C.; Caridroit, M. *Radiolarians in the Sedimentary Record*; Overseas Publishers Association: Amsterdam, 2001.
(9) Kröger, N.; Deutzmann, R.; Sumper, M. *Science* **1999**, *286*, 1129.
(10) Kröger, N.; Lorenz, S.; Brunner, E.; Sumper, M. *Science* **2002**, *298*, 584.
(11) Kröger, N.; Poulsen, N. Diatom Silica Biomineralization: Biochemistry and Molecular Genetics. In *Handbook of Biomineralization: Biological Aspects and Structure Formation*; Bäuerlein, E., Behrens, P., Epple, M., Eds.; Wiley-VCH: Weinheim, 2007.
(12) Poulsen, N.; Sumper, M.; Kröger, N. *Proc. Natl. Acad. Sci. U.S.A.* **2003**, *100*, 12075.
(13) Kröger, N.; Deutzmann, R.; Bergsdorf, C.; Sumper, M. *Proc. Natl. Acad. Sci. U.S.A.* **2000**, *97*, 14133.
(14) Patwardhan, S. V.; Mukherjee, N.; Clarson, S. J. *J. Inorg. Organomet. Polym.* **2001**, *11*, 193.
(15) Patwardhan, S. V.; Maheshwari, R.; Mukherjee, N.; Kiick, K. L.; Clarson, S. J. *Biomacromolecules* **2006**, *7*, 491.
(16) Sewell, S. L.; Rutledge, R. D.; Wright, D. W. *Dalton Trans.* **2008**, 3857.
(17) Kröger, N.; Deutzmann, R.; Sumper, M. *J. Biol. Chem.* **2001**, *276*, 26066.
(18) Wenzl, S.; Hett, R.; Richthammer, P.; Sumper, M. *Angew. Chem., Int. Ed.* **2008**, *47*, 1729.
(19) Rodriguez, F.; Glawe, D. D.; Naik, R. R.; Hallinan, K. P.; Stone, M. O. *Biomacromolecules* **2004**, *5*, 261.
(20) Belton, D.; Paine, G.; Patwardhan, S. V.; Perry, C. C. *J. Mater. Chem.* **2004**, *14*, 2231.
(21) Meegan, J. E.; Aggeli, A.; Boden, N.; Brydson, R.; Brown, A. P.; Carrick, L.; Brough, A. R.; Hussain, A.; Ansell, R. J. *Adv. Funct. Mater.* **2004**, *14*, 31.
(22) Holmstrom, S. C.; King, P. J. S.; Ryadnov, M. G.; Butler, M. F.; Mann, S.; Woolfson, D. N. *Langmuir* **2008**, *24*, 11778.
(23) Degrado, W. F.; Lear, J. D. *J. Am. Chem. Soc.* **1985**, *107*, 7684.
(24) Fu, L.; Liu, J.; Yan, E. C. Y. *J. Am. Chem. Soc.* **2011**, *133*, 8094.
(25) Long, J. R.; Oyler, N.; Drobny, G. P.; Stayton, P. S. *J. Am. Chem. Soc.* **2002**, *124*, 6297.
(26) Mermut, O.; Phillips, D. C.; York, R. L.; McCrea, K. R.; Ward, R. S.; Somorjai, G. A. *J. Am. Chem. Soc.* **2006**, *128*, 3598.
(27) Baio, J. E.; Weidner, T.; Samuel, N. T.; McCrea, K.; Baugh, L.; Stayton, P. S.; Castner, D. G. *J. Vac. Sci. Technol., B* **2010**, *28*, C5D1.
(28) Weidner, T.; Apte, J. S.; Gamble, L. J.; Castner, D. G. *Langmuir* **2010**, *26*, 3433.
(29) Weidner, T.; Breen, N. F.; Li, K.; Drobny, G. P.; Castner, D. G. *Proc. Natl. Acad. Sci. U.S.A.* **2010**, *107*, 13288.
(30) York, R. L.; Holinga, G. J.; Guyer, D. R.; McCrea, K. R.; Ward, R. S.; Somorjai, G. A. *Appl. Spectrosc.* **2008**, *62*, 937.
(31) Nguyen, K. T.; Soong, R.; Lm, S. C.; Waskell, L.; Ramamoorthy, A.; Chen, Z. *J. Am. Chem. Soc.* **2010**, *132*, 15112.
(32) Nguyen, K. T.; King, J. T.; Chen, Z. *J. Phys. Chem. B* **2010**, *114*, 8291.
(33) Baio, J. E.; Weidner, T.; Baugh, L.; Gamble, L. J.; Stayton, P. S.; Castner, D. G. *Langmuir* **2012**, *28*, 2107.
(34) Zane, A. C.; Michelet, C.; Roehrich, A.; Emani, P. S.; Drobny, G. P. *Langmuir* **2014**, *30*, 7152.